

Nanoparticle-Mediated Targeted Therapy With A Novel Tumor Enzyme-Activated Delivery System (TEADS)

Stanley Moffatt^{1,2,*}, Walter Hiddelman³, Mahindra Donarein⁴

1. *Regent University College of Science and Technology, School of Informatics, Engineering and Technology, Accra, Ghana*
2. *University of Texas MD Anderson Cancer Center, Department of Genitourinary Medical Oncology, Laboratory of Experimental Therapeutics, Houston, TX 77030, USA*
3. *University of Texas MD Anderson Cancer Center, Immunopharmacology and Targeted Therapy Section, Department of Bioimmunotherapy and Experimental Therapeutics, Houston, TX 77030, USA*
4. *Tumour Targeting Laboratory, Royal Postgraduate Medical School, Hammersmith Hospital, London, UK.*

**Corresponding author to whom requests for reprints should be addressed, at Regent University College of Science and Technology, School of Informatics, Engineering and Technology, P.O. Box DS 1636, Dansoman, Accra, Ghana.*

ABSTRACT

We describe the design, development and *in vitro* performance of a novel nanoscale platform capable of inducing specific structural modification by enzymatic activity, termed Tumor Enzyme-Activated Delivery System (TEADS). Surface modification allowed the nanoparticle platforms to mimic physiologically inert structures until activation and cleavage by the tumor-specific enzyme, matrix metalloprotease-7 (MMP-7). Two synthesized probes containing distinct fluorescent species and fluorescently labeled cleavable peptide substrate were monitored by gel electrophoresis using quantitative analysis. The model nanoparticles exhibited significant susceptibility to cleavage by MMP-7 at physiological concentrations, with nearly complete cleavage after 24h. This response was MMP-7 enzyme-specific, as cleavage was completely inhibited with increasing molar concentrations of EDTA. The nanoparticle system further combines various attributes for detection, targeting, and payload delivery into a single, multifunctional nanoparticle structure. The successful utilization of MMP-7-specific modification in this TEADS system should have broad implications for tumor-targeted therapy.

INTRODUCTION

One of the most attractive tumor targeting approaches involves the use of molecules capable of activation following cleavage by tumor-specific enzymes (1-3). A number of studies utilizing this approach have focused on the development of tumor-specific molecular imaging constructs cleavable by matrix metalloproteases (MMPs) (4-6).

Matrix metalloproteases including MMP-7, are a family of extracellular, zinc-dependent proteases that have a role in tissue breakdown and remodeling during both normal (*e.g.* angiogenesis) and pathological (*e.g.* inflammation, tumorigenesis) processes. Over-expression of MMP-7 has been directly correlated with enhanced tumorigenicity and tumor cell invasion using *invitro* model systems (7-9) making this enzyme an attractive target for targeted deliveries. Analysis of MMP-7 expression profile has revealed tumor-associated MMP-7 enzyme mRNA, as opposed to the surrounding normal tissue (7-10). This abundant extracellular MMP-7 is expected to provide a potential platform for the *invivo* targeting application of TEADS to cancer targeting. The basis of the MMP-7 specific peptide substrate (RPLALWRS) is employed in this study to impart tumor-specific activity to our nanoparticle (NP) delivery system (8), newly termed in this study as Tumor Enzyme-Activated Delivery Systems (TEADS).

Nanoparticles (NPs) have become a platform of choice due to their large surface area to volume ratio, allowing conjugation of multiple active molecules. Stable covalent conjugation of molecules such as enzymes (11,12), mAbs (13), and peptides (14) to the surface of NPs have been reported. With TEADS, many copies can be attached to the surface of the NP enabling multivalent interaction with target cells, thereby integrating targeted delivery, detection, imaging, and treatment characteristics into a single, multifunctional NP delivery vehicle. In this study, we synthesized and evaluated *invitro* performance of an NP probe capable of specific activation by MMP-7. In addition, the relevance of quantitative analysis of the construct performance is described in the context of *invitro* and *invivo* application. These data provide an empirical basis for a TEADS system capable of targeted and therapeutic payload delivery from a single NP package.

MATERIALS AND METHODS

Nanoparticle (NP) probes and cleavable peptides

A fluorescently labeled, PEGylated substrate for MMP-7 consisting of the cleavable RPLALWRS peptide flanked by polyethylene glycol (PEG) groups of 3400 and 5000g/mol and aminohexanoic acid groups ([Ahx]) to serve as spacer molecules, was synthesized and purified by Anaspec (SanJose, CA). A C-terminal amidation was performed to stabilize the substrate and prevent further modification at this site. The N-terminal amine group of the substrate was conjugated to the surface of carboxylate NPs (585nm emission) using 1-ethyl-3-(3-dimethylaminopropyl)carbodiimide (EDC; Sigma). Briefly, 250 μ l of NPs (7.5 μ M) was diluted to 1mM with 10mM borate buffer, pH 7.4. About 80 μ L from a 10mg/mL stock solution of the cleavable substrate was then added to the solution, yielding a NP-TEADS molar ratio of 10.0:1 (lower bound) and 28.4:1 (upper bound). About 0.57 μ l from a 10mg/ml stock solution of EDC was

added and the mixture was stirred for 2h at room temperature to complete the conjugation. Following conjugation, the mixture was purified by spin filtration, and then buffered with 50mM borate buffer (pH 8.3), before storing the final conjugate at 4°C. The final concentration was determined by measuring the absorbance at 575nm. A schematic of the final NP-TEADS probe is shown in Figure 1 below.

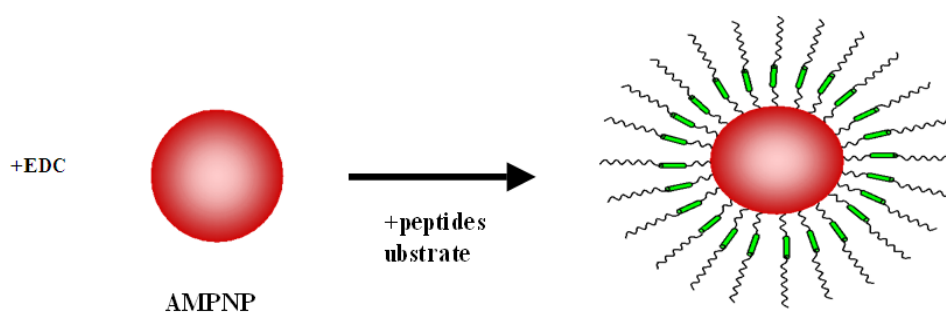


Figure1. Enzyme sensitive NP-TEADS probes were synthesized by surface modification of amphiphilic (AMP) NPs. 5-FAM labeled peptide substrate (green) was synthesized with proximal PEG 3400 and distal PEG 5000 polymers (blacklines). AMP NPs were activated with EDC before addition of the soluble PEGylated substrate. The mixture was stirred for 2h and purified to remove any unreacted components, resulting in a modified, enzyme sensitive NP-TEADS probe (right). This structure enables multivalent interaction of the activated probe with the target site.

Assay for MMP-7 cleavage

To examine the NP and NP-TEADS constructs under enzymatic (MMP-7) activity, active MMP-7 (Calbiochem) was added to 100 μ l of a 50nM TEADS or NP-TEADS solution in borate buffer supplemented with 50 μ M ZnSO₄. The total concentration of MMP-7 was varied in these samples from 100nM to 5nM to reflect expected concentrations *in vivo*. Samples were then incubated at 37°C for various time points ranging from 1h to 48h. Control studies involving NP-TEADS with no enzyme and with inactivated enzyme (by addition of 30mM EDTA, a known zinc chelator) were carried out simultaneously for direct comparison. NP probes were purified from the cleavage products by spin filtration in a 50,000 NMWL cut-off device. Samples were then assayed by gel electrophoresis and spectrofluorometry to determine the extent of construct cleavage from the NP surface.

Analyses of cleavage using gel electrophoresis and quantitative fluorescence

Following the cleavage reaction, NP and NP-TEADS constructs were analyzed on a 10-20% gradient tris-tricine polyacrylamide gel to determine the extent of susceptibility to MMP-7. Unconjugated NP constructs (free in solution) were compared to cleaved NP constructs to straightforwardly visualize and confirm enzymatic activity against the substrate. Gel electrophoresis was also used to monitor the change in electrophoretic mobility of the NP construct. NPs subjected to the

cleavage reaction were assayed against native AMP NPs, uncleaved NP-TEADS constructs, and NP-TEADS + EDTA on a 0.8% buffer-less agarose gel (E-Gel, Invitrogen Corp.). Differences in electrophoretic mobility were used to qualitatively assess construct synthesis (the difference between AMP and NP-TEADS mobilities), construct cleavage (NP-TEADS and cleaved NP-TEADS), and cleavage specificity (cleaved NP-TEADS and NP-TEADS+EDTA). All gels were imaged for fluorescence on a BioDoc-It imaging system (UVP Inc.). Fluorescence spectroscopy (Perkin-Elmer LS 50B) was used to monitor the progress of the cleavage reaction. Prior to experimentation, a fluorescence spectrum of the NP-TEADS construct was taken at 488nm excitation. This spectrum was used to quantify the fluorescence of the labeled TEADS molecules on the NP surface (at 519nm). Following cleavage and purification, the fluorescence spectra of the cleaved NP-TEADS constructs were measured. The peak values at 519nm and 585nm were directly compared to the spectra of control (uncleaved NP-TEADS) particles to estimate the extent of NP construct cleavage following MMP-7 treatment.

Quantitative fluorescence analysis

A quantitative determination of TEADS construct cleavage was made by digital analysis of gel electrophoresis images by banding. The composite intensities were summed to determine the total fluorescence of all bands within each lane. The relative percentage contained in each band was obtained by comparing its composite fluorescence to that of the total for the lane. Fluorescence measurements of NP-TEADS constructs were analyzed to quantitatively determine the extent of NP-TEADS construct cleavage. These quantitative measurements were then scaled to account for the percent of cleavable construct contained in the original sample (from values obtained by quantitative analysis of the polyacrylamide gels previously described).

Statistics

Statistical significance was determined by SigmaStat (Jandel Scientific Software). Differences were termed significant for $p < 0.05$.

RESULTS

The NP-TEADS construct is highly susceptible to cleavage by MMP-7

Gel electrophoresis analysis of unconjugated PA construct confirms specific cleavage of these molecules by MMP-7 (Figure 2). Lanes 1 and 2 confirm the presence of the intact fluorescently labeled NP structure. This cleavage also results in the generation of a very bright high mobility band corresponding to the low molecular weight labeled cleavage product (Figure 2, lanes 3 and 4). NP construct cleavage was completely abolished by the addition of 30mM EDTA (a known zinc chelator; Figure 2, lanes 5 and 6), as the band corresponding to the intact NP construct is present in these wells. These results are consistent with the near complete proteolysis of the NP construct at the site of the MMP target peptide and inhibition of the zinc-dependent MMP-7 enzyme by EDTA.

A quantitative analysis was also made of the gel electrophoresis images obtained from these samples using MATLAB. Table 1 contains representative values obtained from the gel pictured in Figure 2. From these values, we determined the percentage of NP construct contained in each sample. Control, uncleaved soluble NP construct contains $35.6 \pm 3.4\%$ intact NP structure ($n = 4$). After 24h exposure to 100nM MMP-7, $87 \pm 0.7\%$ of the initial NP construct was cleaved (statistically significant, $p < 0.001$) based on the residual $4.6 \pm 0.7\%$ intact NP construct, confirming the high susceptibility of the NP construct to MMP-7 proteolysis. MMP-7 mediated cleavage was completely blocked by the addition of EDTA. After 24h, exposure to 100nM MMP-7 supplemented with 30mM EDTA, $35.5 \pm 2.0\%$ of the PA construct remained intact, a value nearly identical to the amount measured in control samples in the absence of MMP-7 ($p = 0.966$).

Table1. The PEGylated peptide substrate is highly susceptible to cleavage by MMP-7. Cleavage was measured by optical analysis of polyacrylamide gel images. Each band was identified as a region of interest, electronically cut from the image, and loaded into a MATLAB script to calculate the fluorescence intensity for the band. The composite intensity of each well was then calculated by summing the intensities of each constituent band. These results correspond to the gel image in Figure 2. Control, uncleaved NP samples (Lanes 1 and 2) contain an average of 35.7% intact NP structure. 24 hexposure to 100nM MMP-7 results in a reduction of intact NP structure to an average of 4.6%. The percentage of cleavable construct (31.1% average) was then calculated by subtracting the construct remaining after 24h MMP-7 exposure from the average percentage measured in the uncleaved samples. Addition of EDTA to the samples (Lanes 5 and 6) results in strong inhibition of NP construct cleavage, as the percentage of intact construct (35.5% average) is nearly identical to that of control samples in the absence of MMP-7. Quantitative analysis for all experiments ($n \geq 3$) with statistical analysis appears in the Results.

	NP Construct Fluorescence	Total Sample Fluorescence	% Intact NP Construct	% Cleavable NP Construct
Lane1	0.5424	1.3707	39.5%	N/A
Lane2	0.3094	0.9722	31.8%	N/A
Lane3	0.0592	1.1591	5.1%	30.6%
Lane4	0.0607	1.4803	4.1%	31.6%
Lane5	0.3113	0.8443	36.9%	N/A
Lane6	0.3354	0.9852	34.0%	N/A

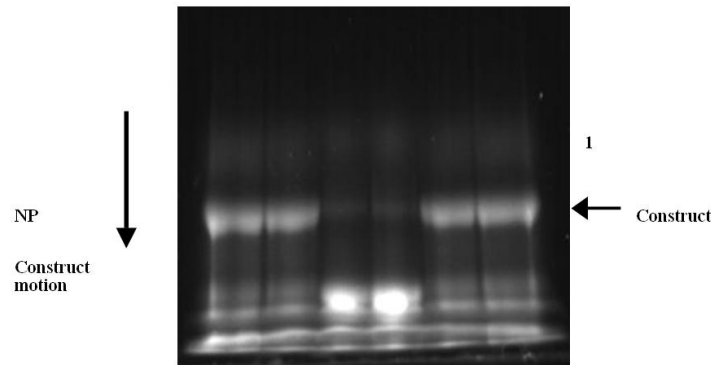


Figure 2. Cleavage of the soluble, unconjugated NP construct by MMP-7 was confirmed by gel electrophoresis. Samples of soluble NP construct were incubated for 24h with 100nM MMP-7 and analyzed on a 10-20% gradient tris-tricine polyacrylamide gel. Lanes 1 and 2 represent unconjugated NP construct prior enzymatic exposure as a control. The bright, low mobility band (identified by the horizontal arrow) represents the intact NP structure, while the other fluorescent bands presumably correspond to unreacted fluorescent species and intermediates not removed during purification. Nearly all of the NP construct is cleaved after 24h exposure to MMP-7 (Lanes 3 and 4). This activity is completely inhibited with the addition of 30mM EDTA (a zinc chelator) to the samples (Lanes 5 and 6). Inhibition of MMP-7 activity results in no measurable cleavage of the NP constructs. The gel pictured is representative of three independent measurements.

Successful modification of NP construct with TEADS

Examination of the electrophoretic mobility of our NP probes was used to determine the success of the surface modification reaction. Figure 3 shows the difference in mobility between unmodified NPs (lanes 3 and 8) and those modified with the TEADS structure (lanes 4 and 9). The resultant NP construct results in a significant increase in MW of the probe and a corresponding decrease in electrophoretic mobility. Following conjugation and purification, the fluorescence spectra of the NP-TEADS constructs were measured (Figure 4, control NP-TEADS). These spectra reveal fluorescence maxima at ~520 and ~590nm, corresponding to the emission maxima of the 5-FAM labeled NP constructs.

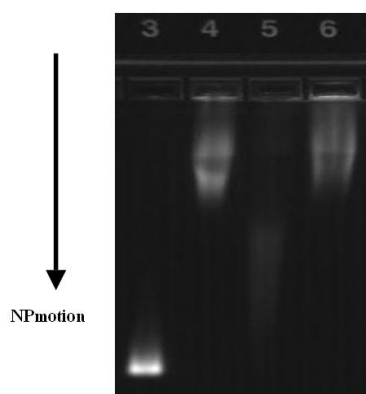


Figure 3. Successful modification of the surface of the NP construct. Electrophoretic mobility of NPs modified with the cleavable NP construct on agarose gel (lane 4, diffuse band) is reduced compared to that of unmodified NPs (lane 3). Twenty four hour exposure of the conjugates to MMP-7 (lane5) leads to a partial recovery of mobility, suggesting significant cleavage of the attached NP structure. Increased mobility after exposure to MMP-7 can be completely inhibited by the addition of 30mM EDTA (lane 6), suggesting the presence of intact NP construct. This image is representative of three independent trials.

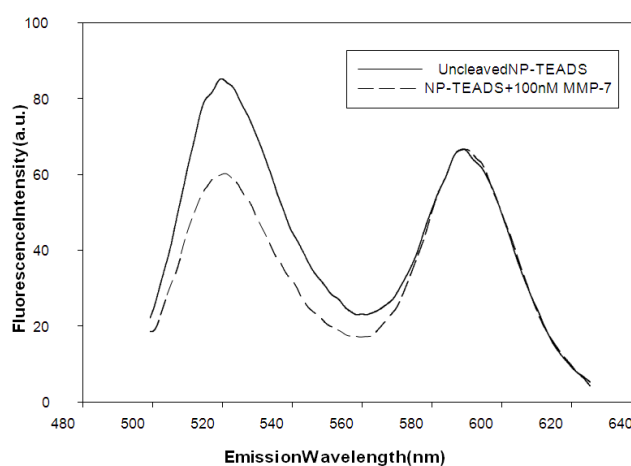


Figure 4. Fluorometric measurements reveal a significant NP cleavage from the construct after 24h exposure to 100nM MMP-7. The presence of two peaks in the uncleaved NP-TEADS also confirms conjugation of the NP construct to surface. Fluorescence spectra of NP-TEADS constructs from 500-625nm were monitored by fluorometry, with an excitation wavelength of 488nm (5nm slit). Spectra were scaled to normalize NP fluorescence intensity (~ 585 nm) among all samples. NPs reacted with TEADS construct and purified to remove unbound material, possess two fluorescence emission peaks consistent with co-localized NP and the construct fluorescence. Exposure to MMP-7 (dashed line) results in reduced 5-FAM fluorescence intensity at ~ 519 nm when compared to control, uncleaved NP-TEADS samples (solid line), suggesting significant cleavage of the labeled NP construct from

the surface at the site of the MMP-7 target substrate. Figure is representative of multiple independent measurements with varying MMP-7 concentrations and incubation times. Results shown are representative of $n \geq 3$ trials for all experimental groups.

NP constructs retain their enzymatic susceptibility after conjugation

MMP-7 mediated increase in electrophoretic mobility is reversed with addition of 30mM EDTA during the cleavage (lanes 6, 11), suggesting inhibition of MMP-7 activity by EDTA. Following the enzymatic exposure, NP constructs were purified from cleavage products by spin filtration, and the fluorescence spectrum of purified NPs was measured (Figure 4). The spectra reveal a reduced fluorescence peak at 519nm corresponding to the labeled, intact NP-TEADS construct.

Fluorescence measurements were used to produce a quantitative analysis of construct cleavage. Treatment of the NP-TEADS constructs with 100nM MMP-7 resulted in steadily increasing cleavage with increased incubation time, reaching a plateau after 24h ($31.8 \pm 5.4\%$ cleavage, $n=3$ for all time points). This scaling revealed nearly complete proteolysis after 24h ($90.9 \pm 15.4\%$ cleavage), consistent with cleavage of unconjugated NP constructs under the same conditions ($87.1 \pm 0.7\%$ cleavage). Results from MMP-7 concentrations ranging from 100nM to 5nM are shown in Figure 5. Although the cleavage response measured for each MMP-7 concentration follows the same general trend, the extent of cleavage is markedly altered, as cleavage declined as MMP-7 concentration was lowered. Furthermore, additional analysis indicated that the initial cleavage rate ($t < 6h$) peaks at an MMP-7 concentration below 100nM, as no additional significant cleavage is measured as enzyme concentration is increased from 10nM to 100nM (data not shown).

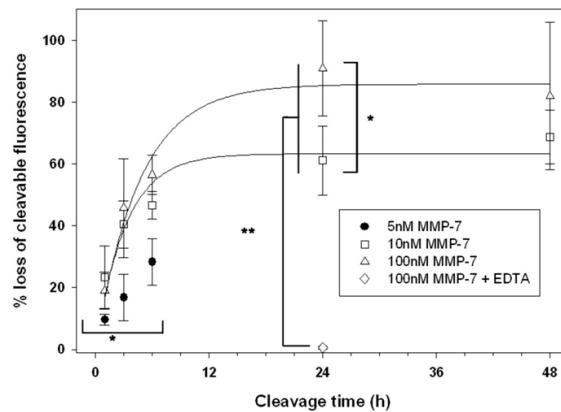


Figure 5. NP-TEADS probes are highly susceptible to MMP-7 activity. Fluorescence spectra of control, uncleaved NP-TEADS structures were compared to those of samples incubated with MMP-7. Fluorescence intensities were then analyzed and scaled to quantitatively determine the extent of proteolytic cleavage of the NP construct from the surface. Measured cleavage was highly dependent on incubation

time, steadily increasing to reach a maximum scaled value of $90.9 \pm 15.4\%$ after 24h incubation with 100nM MMP-7 (hollow triangles). Incubation with 10nM MMP-7 (hollow squares) resulted in reduced cleavage measurements for nearly all time points, although a statistically relevant difference compared to 100nM was only present at 24h. 5nM MMP-7 (solid circles) resulted in statistically reduced cleavage for all time points measured. Cleavage was completely inhibited with the addition of EDTA (solid diamond). The right vertical axis reflects the loss in 5-FAM fluorescence from the NP while the left vertical axis corrects that measurement to yield the percentage of surface-bound PA constructs cleaved. $n \geq 3$ for all concentrations and time points.

DISCUSSION

The present study describes the development and *invitro* performance of novel nanoscale constructs, and demonstrate the feasibility of nanoparticle activation by MMP-7, a proteolytic enzyme secreted by a number of tumors. Cleavage of the internal peptide liberates the distal PEG and part of the peptide (along with a fluorophore, in this work, for assessment of cleavage). Proximity activated targeting not only required the co-localization of the cleavable mask, but also, a fluorescent accessory for performance assessment. The NP-TEADS systems described here minimize undesirable interactions with non-target tissues via a passivating hydrophilic PEG surface coating, as reported previously (15-17). The novel approach described here also employs an active targeting mechanism (cleavage by MMP-7) to activate ligand display only in the vicinity of the target, thus presumably maximizing interaction with target cells. Thus, NP-TEADS constructs may be able to achieve much greater target selectivity over both conventional and single-modality targeted delivery systems.

Traditional gel electrophoresis was utilized to produce some quantitative results. Pixel by pixel optical analysis of polyacrylamide gel data (Figure 2) using MATLAB provided additional insight unavailable by visual inspection alone (Table 1). This analysis revealed that only approximately one-third (~35%) of the original NP construct sample fluorescence is produced by intact NP structure. Fluorometric analysis (Figure 4) confirms the results obtained by gel electrophoresis, verifying both successful conjugation of the NP construct and subsequent cleavage by MMP-7. As each 5-FAM molecule results in lower fluorescence emission intensity than a single NP, this data suggests that multiple NP constructs are conjugated. Subsequent fluorescence spectra taken following MMP-7 cleavage confirm significant cleavage of the intact NP construct, singling out specific MMP-7 mediated activity as the source of reduced fluorescence intensity. At high MMP-7 concentrations (above 100nM), NP-TEADS probes are expected to demonstrate maximal activity reaching significant activity within three hours. The use of NPs as a base for this system imparts desirable characteristics to the composite NP construct, including significant particle mobility and payload delivery.

In this study, even though efforts were made to characterize the efficacy of each targeting strategy (*i.e.* specific homing to target cells and cleavage by a tumor-

specific enzyme), the composite TEADS structure has not yet been synthesized or analyzed. To facilitate construct synthesis, the linking chemistry (N-terminal primary amine) has been conserved between both the targeting and TEADS components. As both constructs utilize the same reaction chemistry and protocol, attachment to the NP surface is expected to occur with similar efficiency. Purification of the final TEADS structure can be conducted by size exclusion using spin filtration as previously described.

The present study forms the basis for a new family of modular nanoscale constructs capable of both targeted therapeutic delivery and sensitive detection of biological phenomena (*e.g.* enzymatic activity). Taken together, our results demonstrate the successful synthesis of a sensitive PEGylated substrate for MMP-7 activity, and its incorporation into a versatile system which displays detection, sensing, targeting and treatment characteristics in a single nanoscale platform. These probes are sensitive to low, physiologically relevant MMP-7 concentrations and represent an alternative approach to small-molecule targeting and systems.

REFERENCES

1. Hallahan DE, Geng L, Cmelak AJ, Chakravarthy AB, Martin W, Scarfone C, Gonzalez A. Targeting drug delivery to radiation-induced neoantigens in tumor microvasculature. *J Control Release* 2001;74(1-3):183-91.
2. Mitra A, Mulholland J, Nan A, McNeill E, Ghandehari H, Line BR. Targeting tumor angiogenic vasculature using polymer-RGD conjugates. *J Control Release* 2005;102(1):191-201.
3. Pastorino F, Brignole C, Marimpietri D, Cilli M, Gambini C, Ribatti D, Longhi R, Allen TM, Corti A, Ponzoni M. Vascular damage and anti-angiogenic effects of tumor vessel-targeted liposomal chemotherapy. *Cancer Res* 2003;63(21):7400-9.
4. Bremer C, Tung CH, Weissleder R. Molecular imaging of MMP expression and therapeutic MMP inhibition. *Acad Radiol* 2002;9 Suppl 2:S314-5.
5. Bremer C, Tung CH, Weissleder R. In vivo molecular target assessment of matrix metalloproteinase inhibition. *Nat Med* 2001;7(6):743-8.
6. McIntyre JO, Fingleton B, Wells KS, Piston DW, Lynch CC, Gautam S, Matrisian LM. Development of a novel fluorogenic proteolytic beacon for in vivo detection and imaging of tumour-associated matrix metalloproteinase-7 activity. *Biochem J* 2004;377(Pt 3):617-28.
7. Wilson CL, Matrisian LM. Matrilysin: an epithelial matrix metalloproteinase with potentially novel functions. *Int J Biochem Cell Biol* 1996;28(2):123-36.
8. Rudolph-Owen LA, Chan R, Muller WJ, Matrisian LM. The matrix metalloproteinase matrilysin influences early-stage mammary tumorigenesis. *Cancer Res* 1998;58(23):5500-6.
9. Yamamoto H, Adachi Y, Itoh F, Iku S, Matsuno K, Kusano M, Arimura Y, Endo T, Hinoda Y, Hosokawa M et al. Association of matrilysin expression

- with recurrence and poor prognosis in human esophageal squamous cell carcinoma. *Cancer Res* 1999;59(14):3313-6.
10. Crawford HC, Scoggins CR, Washington MK, Matrisian LM, Leach SD. Matrix metalloproteinase-7 is expressed by pancreatic cancer precursors and regulates acinar-to-ductal metaplasia in exocrine pancreas. *J Clin Invest* 2002;109(11):1437-44.
 11. Rossi LM, Quach AD, Rosenzweig Z. Glucose oxidase-magnetite nanoparticle bioconjugate for glucose sensing. *Anal Bioanal Chem* 2004;380(4):606-13.
 12. Phadtare S, Vinod VP, Mukhopadhyay K, Kumar A, Rao M, Chaudhari RV, Sastry M. Immobilization and biocatalytic activity of fungal protease on gold nanoparticle-loaded zeolite microspheres. *Biotechnol Bioeng* 2004;85(6):629-37.
 13. Tang D, Yuan R, Chai Y, Liu Y, Dai J, Zhong X. Novel potentiometric immunosensor for determination of diphtheria antigen based on compound nanoparticles and bilayer two-dimensional sol-gel as matrices. *Anal Bioanal Chem* 2005;381(3):674-80.
 14. Liu J, Zhang Q, Remsen EE, Wooley KL. Nanostructured materials designed for cell binding and transduction. *Biomacromolecules* 2001;2(2):362-8.
 15. Akerman ME, Chan WC, Laakkonen P, Bhatia SN, Ruoslahti E. Nanocrystal targeting in vivo. *Proc Natl Acad Sci U S A* 2002;99(20):12617-21.
 16. Ballou B, Lagerholm BC, Ernst LA, Bruchez MP, Waggoner AS. Noninvasive imaging of quantum dots in mice. *Bioconjug Chem* 2004;15(1):79-86.
 17. Gao X, Cui Y, Levenson RM, Chung LW, Nie S. In vivo cancer targeting and imaging with semiconductor quantum dots. *Nat Biotechnol* 2004;22(8):969-76.

